ISSN 1674-1056
http://cpb.iphy.ac.cn
http://iopscience.iop.org/cpb
中国物理 B
Chinese Physics
中国物理 Chinese Physics B

Effects of the band-filling and Fe/Mo disorder on physical properties of Ca_2FeMoO_6

Jin-Feng Wang(王金凤), Zhao-Tong Zhuang(庄照通), Shuai-Shuai Liu(刘帅帅), Qian-Qian Gao(高迁迁)

Citation: Chin. Phys. B . 2018, 27(12): 127201. **doi:** 10.1088/1674-1056/27/12/127201
Journal homepage: http://cpb.iphy.ac.cn; http://iopscience.iop.org/cpb

What follows is a list of articles you may be interested in

Spin-independent transparency of pure spin current at normal/ferromagnetic metal interface

Runrun Hao(郝润润), Hai Zhong(钟海), Yun Kang(康韵), Yufei Tian(田雨霏), Shishen Yan(颜世申), Guolei Liu(刘国磊), Guangbing Han(韩广兵), Shuyun Yu(于淑云), Liangmo Mei(梅良模), Shishou Kang(康仕寿)

Chin. Phys. B . 2018, 27(3): 037202. **doi:** 10.1088/1674-1056/27/3/037202

Nonvolatile control of transport and magnetic properties in magnetoelectric heterostructures by electric field

Qian Li(李潜), Dun-Hui Wang(王敦辉), Qing-Qi Cao(曹庆琪), You-Wei Du(都有为)

Chin. Phys. B . 2017, 26(9): 097502. **doi:** 10.1088/1674-1056/26/9/097502

The origin of spin current in YIG/nonmagnetic metal multilayers at ferromagnetic resonance

Yun Kang(康韵), Hai Zhong(钟海), Runrun Hao(郝润润), Shujun Hu(胡树军), Shishou Kang(康仕寿), Guolei Liu(刘国磊), Yin Zhang(张引), Xiangrong Wang(王向荣), Shishen Yan(颜世申), Yong Wu(吴勇), Shuyun Yu(于淑云), Guangbing Han(韩广兵), Yong Jiang(姜勇), Liangmo Mei(梅良模)

Chin. Phys. B . 2017, 26(4): 047202. **doi:** 10.1088/1674-1056/26/4/047202

Spin transport in a Zigzag normal/ferromagnetic graphene junction

Shi Hao-Sheng, Vahram L. Grigoryan

Chin. Phys. B . 2015, 24(5): 057202. **doi:** 10.1088/1674-1056/24/5/057202

Spin-polarized injection into p-type GaAs layer from a Co_2MnAl injector

Yuan Si-Peng, Shen Chao, Zheng Hou-Zhi, Liu Qi, Wang Li-Guo, Meng Kang-Kang, Zhao Jian-Hua

Chin. Phys. B . 2013, 22(4): 047202. **doi:** 10.1088/1674-1056/22/4/047202

Effects of the band-filling and Fe/Mo disorder on physical properties of Ca_2FeMoO_6*

Jin-Feng Wang(王金凤)†, Zhao-Tong Zhuang(庄照通), Shuai-Shuai Liu(刘帅帅), and Qian-Qian Gao(高迁迁)

College of Physics and Materials Science, National Demonstration Center for Experimental Physics Education, Henan Normal University and Henan Key Laboratory of Photovoltaic Materials, Xinxiang 453007, China

(Received 1 August 2018; revised manuscript received 2 October 2018; published online 25 November 2018)

Both the band filling effect and Fe/Mo disorder have a close correlation with the physical properties of the double perovskite Ca_2FeMoO_6. Two series of Ca_2FeMoO_6 and $Nd_{0.3}Ca_{1.7}FeMoO_6$ ceramics sintered at (1050 °C, 1200 °C, and 1300 °C) were specially designed to comparatively investigate the band-filling effect and Fe/Mo disorder on the physical properties of Ca_2FeMoO_6. The x-ray diffraction indicates that Fe/Mo disorder is sensitive to the sintering temperature. The magnetization behavior is mainly controlled by the Fe/Mo disorder not by the band filling effect, manifested by a close correlation of saturated magnetization (M_s) with the Fe/Mo disorder. Interestingly, magnetoresistance (MR) property of the same composition is dominantly contributed by the grain boundary strength, which can be expressed by the macroscopic resistivity values. However, the band filling effect caused by the Nd-substitution can decrease the spin polarization, and thus suppress the MR performance fundamentally. Contrary to the MR response, the Curie temperature (T_C) shows an obvious optimization due to the band filling effect, which increases the carrier density near the Fermi level responsible for the ferromagnetic coupling interaction strengthen. Maybe, our work can provoke further research interests into the correlation of the band-filling effects and Fe/Mo disorder with the physical properties of other Fe/Mo-based double perovskites.

Keywords: band filling effect, Fe/Mo disorder, Ca_2FeMoO_6, physical property

PACS: 72.25.Mk, 75.47.Gk **DOI:** 10.1088/1674-1056/27/12/127201

1. Introduction

As a representative of the strongly correlated systems, double perovskite Sr_2FeMoO_6 (SFMO) has been paid a great deal of attention. Because it has a considerable high low-field magnetoresistance (LFMR) behavior, a half-metal nature with 100% spin-polarization, and a high T_C well above room temperature.[1–4] Those functional properties will make FeMo-based double perovskites systems (A_2FeMoO_6, A: Ca/Sr/Ba) become promising candidates from both fundamental investigations and potential technological applications in spintronics and magnetic storage devices operated at room temperature.[1,2,5]

In an ideal A_2FeMoO_6 (A: Ca/Sr/Ba) structure, the electron configuration can be originally addressed as the localized spin-up electrons of the $3d^5$ (Fe^{3+}) and the itinerant spin-down electron of the $4d^1$ (Mo^{5+}) shared by the $Fe^{3+}(t_{2g}\downarrow)-O(2p)-Mo^{5+}(t_{2g}\downarrow)$ subband.[5,6] Localized five electrons of Fe^{3+} ($3d^5$, $S=5/2$) antiferromagnetically couple with one electron contributed by Mo^{5+} ($4d^1$, $S=1/2$), resulting in a net magnetization of $4\mu_B$/f.u.[7,8] However, a much lower magnetization is commonly reported in the experiments since the inevitable Fe/Mo anti-site defects (ASD) occurs, *i.e.*, Fe occupies Mo positions wrongly and *vice versa*.[7,9–11] ASD has a close correlation with magnetization. Additionally, theoretical works predicate that ASD significantly influences the electron spin polarization near Fermi level and even can destroy the half-metal property when exceeding a certain concentration.[12,13] Hence, controlling ASD content is crucial for investigating the physical property in FeMo-based double perovskites. The itinerant electron at conduction band is suggested to mediate the ferromagnetic interaction between neighbor Fe cations by a double-exchange-like mechanism.[14–16] Indeed, substituting the divalent A^{2+} ions in A_2FeMoO_6 (A: Sr^{2+}/Ba^{2+}) with the trivalent ions (such as La^{3+}, Nd^{3+}), a significantly improved T_C can be observed due to the increased electron density.[6,17–20] Although these observations did disclose a positive correlation between ferromagnetic couplings strength and the carrier density near Fermi level, it cannot show the unique contribution of the band filling effect. In those electron-doped systems, the ionic sizes of the Sr^{2+}/Ba^{2+} (1.26/1.42 Å) strongly differ from the substituting cations La^{3+}/Nd^{3+} (1.16/1.109 Å), electron dopings not only provide the carrier into the conduction band but also trigger a rotation of (Fe, Mo)O_6 octahedra.[6,17–19] The rotation will change the Fe–O–Mo band angle, even reduce the crystal symmetry and consequently modify the carrier density at the Fermi level.[6,17–19] In order to provide a relatively clean research environment, we select $Nd_{0.3}Ca_{1.7}FeMoO_6$ as the research object because of the well-matched ionic sizes of Nd^{3+} (1.109 Å) and Ca^{2+} (1.12 Å), which can avoid the steric ef-

*Project supported by the National Natural Science Foundation of China (Grant No. U1504107) and the Doctoral Scientific Research Foundation (Grant No. qd15214).

†Corresponding author. E-mail: jfwang@htu.edu.cn

© 2018 Chinese Physical Society and IOP Publishing Ltd

fects effect as far as possible. Through the above analysis, both the band filling effect caused by the electron doping and ASD significantly function on the physical properties of the FeMo-based double perovskites. Therefore, it is interesting to comparatively investigate two effects on physical properties.

In this work, three groups of single-phased pristine Ca_2FeMoO_6 (CFMO) and $Nd_{0.3}Ca_{1.7}FeMoO_6$ (NCFMO) ceramics were prepared at various sintering temperature (1050 °C, 1200 °C, and 1300 °C). The corresponding crystal structure, magnetization, resistivity, magnetoresistance, and the T_C were systematically and comparatively investigated.

2. Experimental

2.1. Samples synthesis

For clarity and simplicity, the CFMO ceramics were synthesized at various sintering temperature (1050 °C, 1200 °C, 1300 °C), which were labeled as C1, C3, C5. At the same sintering temperature, the NCFMO ceramics were also prepared, which were denoted as C2, C4, C6, respectively. Each group of (C1, C2), (C3, C4), (C5, C6) has the same sintering temperature. All the above-mentioned ceramics were prepared via the solid-state reaction process. Frist, the dried raw materials of Nd_2O_3, $CaCO_3$, Fe_2O_3, and MoO_3 ($\geq$ 99.5%) were weighted, mixed homogeneously by balling milling in ethanol for 24 h, and the slurry was dried. The dried powders were calcined at 800 °C in air for 10 h. Then, the calcined mixtures were ball milled in ethanol for another 24 h, dried and pressed into small thin disks (10 mm×1 mm). Finally, all the disks were sintered at three different temperatures (1050 °C, 1200 °C, 1300 °C) for 8 h in a reducing atmosphere of a mixed gas of 10% H_2/90% Ar.

2.2. Characterization

The structures of the samples were confirmed by x-ray diffraction (XRD) patterns (XRD, Bruker D8 Discover). The microstructures were investigated through a field emission scanning electron microscope (FESEM, Zeiss SUPRA 40). The magnetic and transport data were obtained through a superconducting vibrating sample magnetometer (VSM) and a physical property measurements system (PPMS Quantum Design, 2001NUGC).

3. Results and discussions

The normalized XRD patterns of all samples are shown in Fig. 1(a). It can be clearly seen that all the diffraction peaks are well consistent with double perovskite structure with a monoclinic phase and a space group of $P2_1/n$ and no second phase is detectable,[21–25] which means that the C1–C6 samples are single-phased. The superstructure diffracted peaks of {110} resulting from the ordered arrangement of Fe and Mo cations at the B-sites are particularly sensitive to Fe/Mo ordering degree.[25] Similar to the Fe/Mo ordering degree in SFMO, the Fe/Mo ordering degree in CFMO can be expressed by the relative intensity ratio of $I\{110\}/\{I(020)+I(112)\}$ qualitatively.[8] The variance of $I\{110\}/\{I(020)+I(112)\}$ of C1–C6 as a function of the sintering temperature are plotted in Fig. 1(b). One can see clearly that, either maternal CFMO (C1, C3, C5) or NCFMO (C2, C4, C6), $I\{110\}/\{I(020)+I(112)\}$ relative ratio improve with increasing sintering temperature. The experimental observation is consistent with data reported in FeMo-based double perovskites,[7,26] confirming that manipulating the sintering temperature is a facile and efficient strategy to control the Fe/Mo ordering degree (contrary to Fe/Mo ASD). Interestingly, for each sintering temperature, $I\{110\}/\{I(020)+I(112)\}$ relative ratio of the NCFMO (C2, C4, C6) ceramics is slightly less than that of the CFMO (C1, C3, C5), respectively. It indicates that Nd-substitution in CFMO has no obvious decrease of the Fe/Mo ordering degree. This is vastly different from the La-doped Sr_2FeMoO_6 systems, where, the Fe/Mo ordering degree shows a remarkable decrease upon the increase of La-doping content.[6,18,27] The difference between them may attribute to the close ion sizes of Nd/Ca cations. The ordering degree of Fe/Mo (Fe/Mo ASD) has a close correlation with the magnetization, which will be discussed in the Fig. 2 in detail.

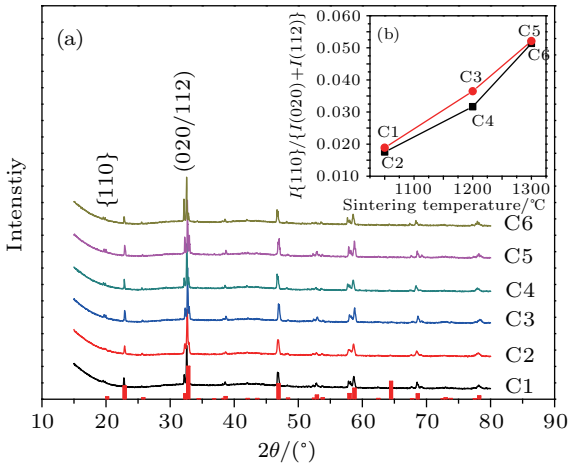


Fig. 1. (color online) (a) All the XRD patterns of C1–C6 samples. (b) The ratio of the $I\{110\}/\{I(020)+I(112)\}$ as a function of the sintering temperature.

The M–H curves of C1–C6 ceramics measured at 50 K are present in Figs. 2(a)–2(c). It can be distinctly observed that all the samples show well-saturated hysteresis loops with a small coercive field, indicating a typical soft ferromagnetic behavior.[28–30] The saturated magnetization (M_s) as a function of the sintering temperature curve is showed in Fig. 2(d). By comparing the Fig. 1(b) and Fig. 2(d), the varied trend of M_s with the sintering temperature is in accordance with that of the relative ratio of the $I\{110\}/\{I(020)+I(112)\}$ manifesting the main contribution of the Fe/Mo ordering degree to the

magnetization. The reasons lie in that, once Fe/Mo ASD occurs, giving rise to antiferromagnetic –Fe–O–Fe–O– patches and paramagnetic –Mo–O–Mo–O– patches between ordering ferromagnetic domains.[7,31] Actually, a great deal of experimental results confirmed that both patches can greatly weaken the magnetization in FeMo-based double perovskites.[7,9,30] As for the origin of the less M_s of (C2, C4, C6) than (C1, C3, C5), there are two possible reasons: one is Nd-substitution will bring about intrinsic Fe/Mo defect in spite of close ion sizes of Nd/Ca cations; the other is the band filling effect caused by the electron injection at conduction band. Based on the above analysis, the magnetization is mainly controlled by the Fe/Mo ASD, whereas we cannot completely conclude the minor negative contribution of the band filling effect.

Generally, prepared process drastically affect the macroscopic structures of the ceramics, such as grain sizes, grain density, the connectivity between grains, grain boundary numbers, grain boundary strength and so on, which can strongly influence on the electrical transport, magnetoresistance, chemical states and other physical properties. Hence, the surface structures of C1–C6 are analyzed by SEM images as shown in Figs. 3(a)–3(f). As for maternal CFMO ceramics (Figs. 3(a)–3(c)), both the grains sizes and connectivity of (C1, C3, C5) improve significantly with increasing sintering temperature. The similar experimental phenomenon can be observed for Nd-doped CFMO (C2, C4, C6). The possible reasons may lie in that, high sintering temperature favors for promoting grain growth and improving connectivity between nearby grains. So the microstructures variance of all the ceramics is reasonable. Additionally, based on previous experimental data, the ceramic formed with a larger grain size and more close connectivity will show a reduced resistivity,[30] which will be discussed as below.

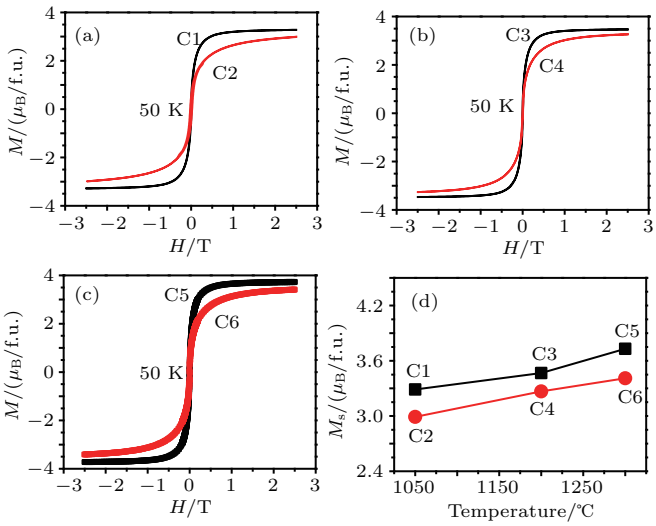


Fig. 2. (color online) Magnetic hysteresis loops (M–H) at 50 K for (a) C1, C2; (b) C3, C4, and (c) C5, C6. (d) The saturated magnetization (M_s) curves as a function of the sintering temperature for all the samples.

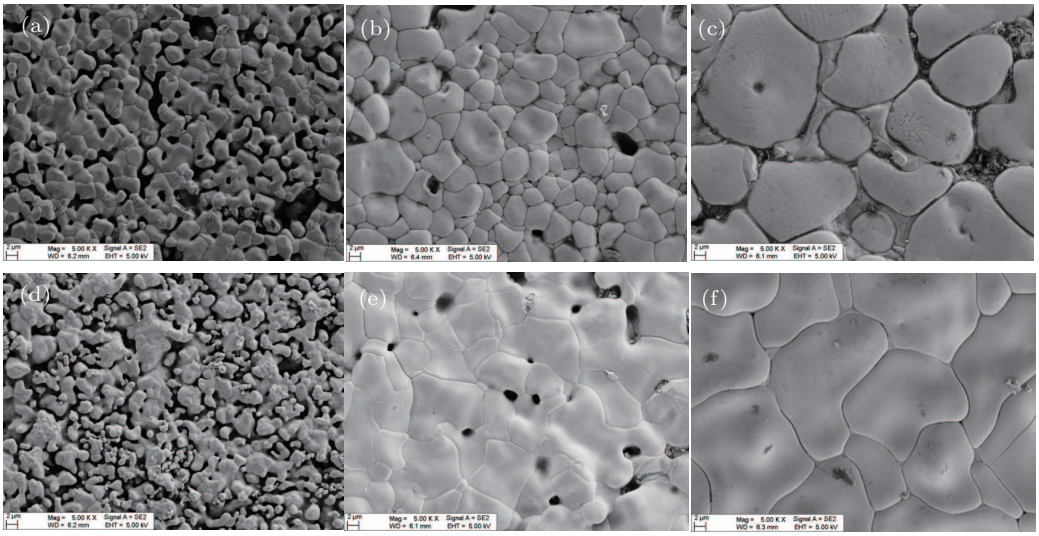


Fig. 3. (color online) (a)–(c) Typical SEM images of (C1, C3, C5) and (d)–(f) (C2, C4, C6) ceramics.

The temperature-dependent resistivity (ρ–T) without and with a magnetic field of 2 T, and the temperature-dependent magnetoresistance (MR-T) curves for all the ceramics are shown in Figs. 4(a)–4(f), respectively. The resistivity of maternal CFMO ceramics (C1, C3, C5) decrease gradually with increasing the sintering temperature, and the similar tendency can be observed in Nd-doped CFMO ceramics (C2, C4, C6), which may be contributed by different macroscopic structures as displayed in Fig. 3. The negative magnetoresistance (MR) effect is a decrease of the electrical resistance in response to an applied magnetic field. In FeMo-based on double perovskites, it is confirmed that the MR effect is dominantly controlled by the grain boundary strength (GBs), which can be qualitatively expressed by the macroscopic resistivity.[32–34] Generally, the GBs are contributed by the energy barrier Δ and the width s of the GB insulating barriers, the macroscopic physical pa-

rameters of GB, such as the connectivity, number, grain size, structural defects and local density of states can be included in parameters of s and Δ. The relation between resistivity and GB strength can be expressed as $\rho \infty \exp(\gamma s\sqrt{\Delta})$, where γ is a constant parameter. In general, for a given composition, the ceramic with a larger resistivity will display higher MR at the same measured conditions.[26,33–35] It is interesting to find that the resistivity of C1 shows a sharp decrease under an external magnetic field of $H = 2$ T. Such a changed magnitude weakens gradually with increasing measured temperature, indicating a strong correlation of negative MR behavior with the temperature (the right y axis). The MR effect of maternal CFMO ceramics (C1, C3, C5) are suppressed by the increasing sintering temperature. For example, the MR% of C1, C3, and C5 at 50 K are −27.5%, −13.7%, and −8.17%, respectively. The diminished resistivity values of (C1, C3, C5) predicate the decreased grain boundary strength, leading to a suppressed MR effect as shown in Figs. 4(a)–4(c). Actually, the similar MR behavior can be found in (C2, C4, C6) ceramics.

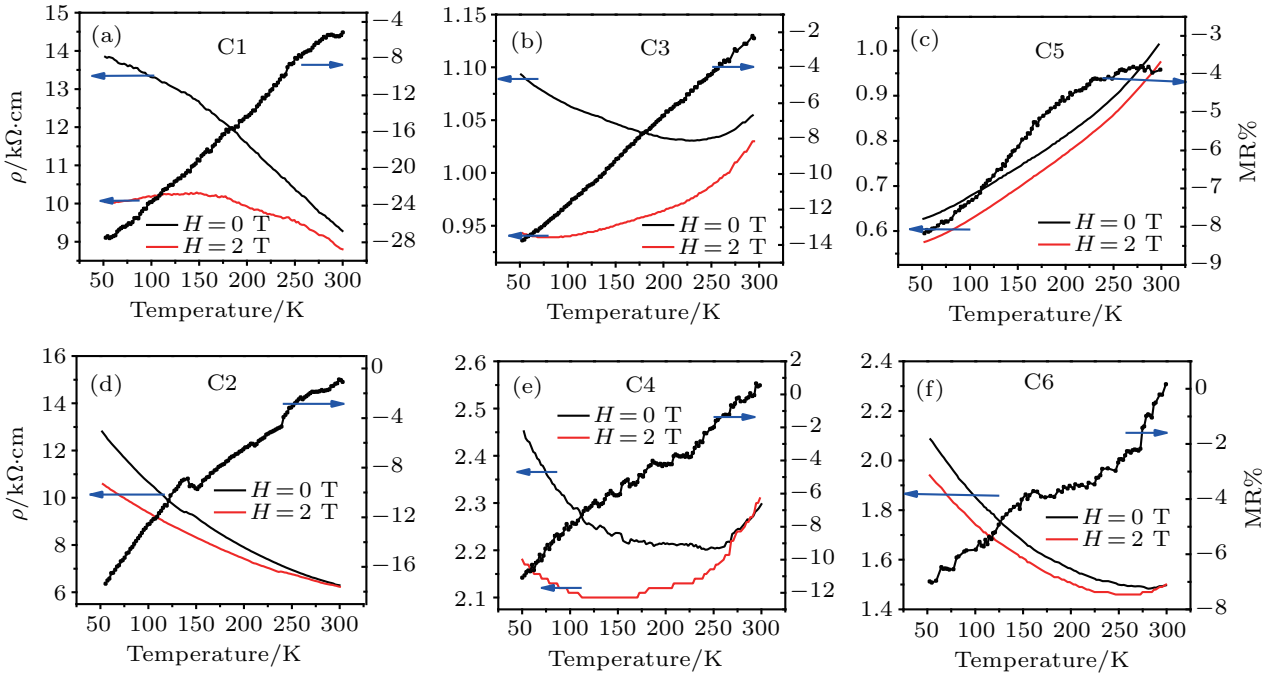


Fig. 4. (color online) Temperature-dependent resistivity (ρ–T, the left y axis) without and with a magnetic field of 2 T, temperature-dependent MR curves (the right y axis) of C1–C6.

The temperature-dependent MR behaviors under a magnetic field of 2 T have been investigated in Fig. 4. The response of the MR to the varied magnetic field is also important for practical applications. Therefore, the MR of C1–C6 as a dependence of the magnetic field (MR–H) curves obtained at 50 K and 300 K are plotted in Fig. 5 and Fig. 6, respectively. Here, The MR% is defined as: $\mathrm{MR}\% = (\rho_H - \rho_0) \times 100\%/\rho_0$, where ρ_H and ρ_0 are the resistivity with and without the external field. From Figs. 5(a)–5(c), mainly three aspects of MR with respect to H can be expressed. The first is that all the samples show a typical characteristic of the LFMR behavior,[1,35] *i.e.*, negative MR increases deeply at low field ($H \leq 1$ T), whereas increases relatively smoothly at high field ($H > 1$ T). Moreover, such an LFMR property of C5 and C6 deteriorates drastically. The second is that, both (C1, C3, C5) and (C2, C4, C6) ceramics display a weakened LFMR effect with improved sintering temperature (Fig. 5(d)). The temperature-dependent LFMR behavior is contrary to the magnetization response as discussed in Fig. 2, whereas consistent with the tendency of resistivity with the sintering temperature. The sharp contrast indicates that LFMR in the research objects is dominantly controlled by the grain boundary effect not by ASD content. Additionally, the observed temperature-dependent LFMR nature convincingly predicates that lowering the sintering temperature is an efficient experimental strategy of optimizing the MR performance. A considerable LFMR ($H = 1$ T) of −22.5% can be obtained in C1, which is much larger than the reported approximately −12.5% in maternal CFMO ceramics.[23] The third, LFMR values of (C1, C3, C5) are superior to that of the Nd-doped CFMO (C2, C4, C6) ceramics at the same sintering temperature. This result is in accordance with the similar electron-doped FeMo-based double perovskites.[8,23,36] The possible reasons lie in that, the band filling effect contributed by Nd-substitution will bring about the injection of the electron at conduction band, and resulting in the decreased spin polarization of electron near Fermi level, and then a decreased MR property.[8,36] Actually, MR property of C1–C6 measured at 300 K exhibit a similar behavior (Fig. 6).

The field-cooling (200 Oe, 1 Oe = 79.5775 A·m^{-1}) magnetization-temperature (M–T) curves of C1–C6 are shown in Figs. 7(a)–7(c). All the ceramics transited from a paramagnetic state to a ferromagnetic state with decreasing the temperature.[29] The T_C, indicated by an abrupt drop in the magnetization to zero, which can be estimated from the inflection point of M–T curves.[6,29] One can clearly see that, all the ceramics exhibit a well-above room temperature T_C values (Fig. 7(d)), and the T_C values of Nd-doped C2, C4, and C6 are higher than that of C1, C3, and C5, respectively. The observation is contrary to the magnetization response, manifesting minor role of the Fe/Mo ASD on the T_C values. Although the spin polarization of electron at Fermi level decrease because of the band filling effect, giving rise to the increased carrier density near the Fermi level, which is proposed to has a positive ferromagnetic coupling strength.[6,18,19,23,30] The carrier density of the Nd-doped C2, C4, and C6 is higher than that of maternal CFMO ceramics (C1, C3, C5), then resulting in an improved ferromagnetic interaction strength and an optimized T_C values.

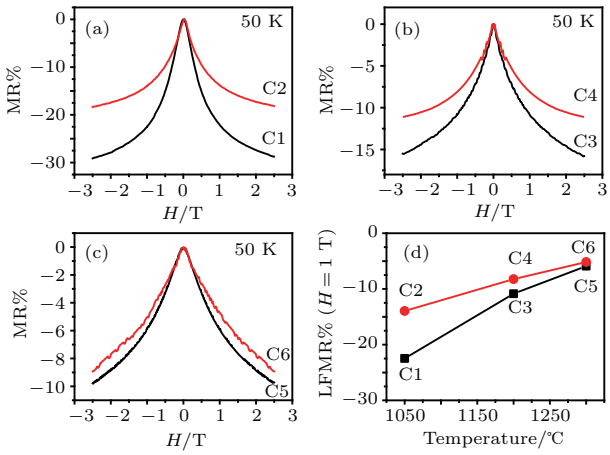


Fig. 5. (color online) Magnetoresistance as a function of the magnetic field (MR–H) curves at 50 K for (a) C1, C2; (b) C3, C4, and (c) C5, C6. (d) LFMR% at 1 T for C1–C6 as a function of the sintering temperature.

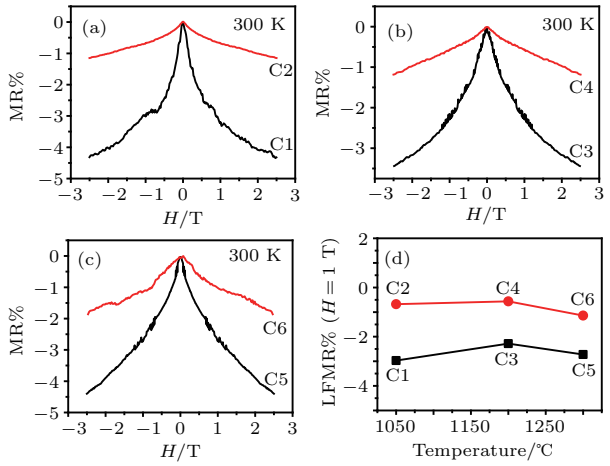


Fig. 6. (color online) MR–H curves of (a) C1, C2; (b) C3, C4, and (c) C5, C6 at 300 K. (d) LFMR% at 1 T for C1–C6 as a function of the sintering temperature.

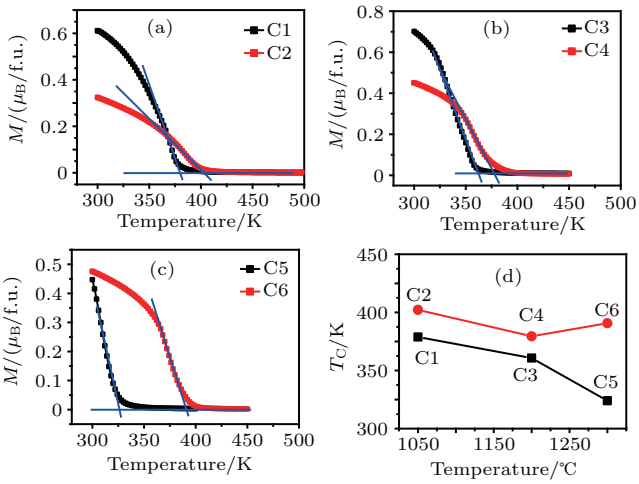


Fig. 7. (color online) Temperature-dependent magnetization (M–T) curves for (a) C1, C2; (b) C3, C4, and (c) C5, C6. (d) Evolution of the Curie temperature (T_C) as a dependence of the sintering temperature.

4. Conclusions

Two series of CFMO (C1, C3, C5) and NCFMO (C2, C4, C6) ceramics sintered at (1050 °C, 1200 °C, 1300 °C) have been specially designed to comparatively investigate the band-filling effect and Fe/Mo ASD on the physical properties of CFMO. The x-ray diffraction indicates that Fe/Mo ASD can be effectively tuned by controlling the sintering temperature. A consistent varied trend of the M_s with the Fe/Mo ASD manifests that the magnetization behavior is mainly controlled by the Fe/Mo ASD not by the band filling effect. Interestingly, magnetoresistance (MR) property of a given composition is dominantly contributed by the grain boundary strength, which can be expressed by the macroscopic resistivity values. However, the band filling effect caused by the Nd-substitution can decrease the spin polarization, and thus suppress MR performance fundamentally. Compared to the maternal CFMO ceramics, a considerable improved T_C can be observed in NCFMO ceramics since the band filling effect can increase the carrier density near Fermi level, which is responsible for the ferromagnetic coupling interaction strength. Maybe, our work can provoke further investigations interest into the correlation of the band-filling effects and Fe/Mo disorder with the physical properties of other Fe/Mo-based double perovskites.

References

[1] Kobayashi K I, Kimura T, Sawada H, Terakura K and Tokura Y 1998 *Nature* **395** 677
[2] Pickett W E and Moodera J S 2001 *Phys. Today* **54** 39
[3] Wang J F , Zhuang Z T , Liu S S , Shi T F and Jia Z J 2018 *J. Phys. D: Appl. Phys.* **51** 258003
[4] Erten O, Meetei O N, Mukherjee A, Randeria M, Trivedi N and Woodward P 2013 *Phys. Rev. B* **87** 165105
[5] Serrate D, De Teresa J and Ibarra M 2007 *J. Phys.: Condens. Matter* **19** 023201
[6] Navarro J, Frontera C, Balcells L, Martínez B and Fontcuberta J 2001 *Phys. Rev. B* **64** 092411
[7] Huang Y H, Linden J, Yamauchi H and Karppinen M 2004 *Chem. Mater.* **16** 4337

[8] Balcells L L, Navarro J, Bibes M, Roig A, Martı´nez B and Fontcuberta J 2001 *Appl. Phys. Lett.* **78** 781

[9] Wang J F, Xu X J, Ji W J, Zhang S T, Zhou J, Gu Z B, Chen Y, Yuan G L, Yao S H and Chen Y F 2013 *CrystEngComm* **15** 4601

[10] Panguluri R P, Xu S, Moritomo Y, Solovyev I V and Nadgorny B 2009 *Appl. Phys. Lett.* **94** 012501

[11] Reyes A M, Arredondo Y and Navarro O 2016 *J. Phys. Chem. C* **120** 4048

[12] Sahadasgupta T and Sarma D D 2001 *Phys. Rev. B* **64** 064408

[13] Singh V N and Majumdar P 2011 *Europhys. Lett.* **94**

[14] Sanyal P and Majumdar P 2009 *Phys. Rev. B* **80** 1956

[15] Ray S, Kumar A, Sarma D D, Cimino R, Turchini S, Zennaro S and Zema N 2001 *Phys. Rev. Lett.* **87** 097204

[16] Yang D, Harrison R J, Schiemer J A, Lampronti G I, Liu X, Zhang F, Ding H, Liu Y g and Carpenter M A 2016 *Phys. Rev. B* **93** 024101

[17] Rubi D, Frontera C, Nogués J and Fontcuberta J 2004 *J. Phys.: Condens. Matter* **16** 3173

[18] Frontera C, Rubi D, Navarro J, García-Muñoz J L, Fontcuberta J and Ritter C 2003 *Phys. Rev. B* **68** 012412

[19] Yang H M, Lee W Y, Han H, Lee B W and Kim C S 2003 *J. Appl. Phys.* **93** 6987

[20] Hussain I, Anwar M S, Kim J W, Chung K C and Koo B H 2016 *Ceram. Int.* **42** 13098

[21] Poddar A, Bhowmik R N and Muthuselvam I P 2010 *J. Appl. Phys.* **108** 8905

[22] Muthuselvam I P, Poddar A and Bhowmik R N 2009 *J. Alloys Compd.* **486** 536

[23] Rubi D, Frontera C, Fontcuberta J, Wojcik M, Jedryka E and Ritter C 2004 *Phys. Rev. B* **70** 094405

[24] Rubi D 2004 *J. Appl. Phys.* **95** 7082

[25] Rubi D, Nogués J, Muñoz J S and Fontcuberta J 2006 *Mater. Sci. Eng. B* **126** 279

[26] Wang J F and Zhang Y M 2017 *Mater. Res. Bull.* **90** 145

[27] Jana S, Meneghini C, Sanyal P, Sarkar S, Saha-Dasgupta T, Karis O and Ray S 2012 *Phys. Rev. B* **86**

[28] López-Ortega A, Estrader M, Salazar-Alvarez G, Roca A G and Nogués J 2015 *Phys. Rep.* **553** 1

[29] Wang J F, Zhuang Z T, Shi T F, Gao Q Q and Jia Z J 2018 *Ceram. Int.* **44** 8492

[30] Wang J, Song X, Li Y and Zhuang Z 2017 *Ceram. Int.* **43** 5585

[31] Nieves Menéndez, Mar Garcíahernández, Diana Sánchez J D T, J L M, and Alonso J A 2004 *Chem. Mater.* **16** 3565

[32] Niebieskikwiat D, Caneiro A, Sánchez R D and Fontcuberta J 2001 *Phys. Rev. B* **64** 180406

[33] Niebieskikwiat D, Prado F, Caneiro A and Sánchez R D 2004 *Phys. Rev. B* **70** 132412

[34] Wang J F, Hu B, Zhang J, Gu Z B and Zhang S T 2015 *J. Alloys Compd.* **621** 131

[35] Wang J F, Li Z, Xu X J, Gu Z B, Yuan G L and Zhang S T 2014 *J. Am. Ceram. Soc.* **97** 1137

[36] Rubi D and Fontcuberta J 2006 *J. Phys.: Condens. Matter* **18** 7991